New plutonium isotope: ^{231}Pu

C. A. Laue, K. E. Gregorich, R. Sudowe,* M. B. Hendricks, J. L. Adams, M. R. Lane, D. M. Lee, C. A. McGrath, D. A. Shaughnessy, D. A. Strellis, E. R. Sylwester, P. A. Wilk, and D. C. Hoffman

Nuclear Science Division, MS 70A-3307, Lawrence Berkeley National Laboratory, One Cyclotron Road, Berkeley, California 94720

(Received 24 December 1998)

The new plutonium isotope, ^{231}Pu, was produced by the ^{233}U(^{3}He,5n)^{231}Pu reaction. After chemical separation, the ^{231}Pu decay modes were studied using α-spectrometry. The isotope, ^{231}Pu, was unequivocally identified by the α-decay of the chain members from its α- and electron-capture daughters using the α-α-correlation technique. The half-life of ^{231}Pu was determined to be (8.6 ± 0.5) min. An α-group with an energy of (6.72 ± 0.03) MeV was assigned to ^{231}Pu. [S0556-2813(99)03406-8]

PACS number(s): 27.90.+b, 21.10.Tg, 23.60.+e, 25.55.−e

I. INTRODUCTION

Soon after plutonium's initial discovery in 1941, researchers associated with Glenn T. Seaborg's group started to explore the neutron-deficient plutonium isotopes. In 1951, Orth [1] discovered ^{232}Pu, the lightest plutonium isotope known at that time, and remaining so for nearly 40 years. In 1957, Thomas *et al.* [2] identified ^{233}Pu. In 1972, Jäger *et al.* [3] restudied the plutonium isotopes 232 to 234. Essentially, they confirmed the previous data, but provided more accurate measurements of half-lives and α-decay energies (see Table I). Nevertheless, questions still remain concerning the reported ^{232}Pu α-decay energies. In order to provide a rapid separation of plutonium, neptunium was not removed from the plutonium fraction even though the neptunium decay chains interfere strongly with investigations of the plutonium decay.

The study of the radioactive properties of neutron-deficient actinides, in particular the systematics of α- and orbital electron-capture (EC) decay properties, is still of intrinsic interest. The discovery of previously unknown isotopes contributes to our understanding of α-decay systematics and half-lives, and leads to more precise values of atomic masses, neutron and proton binding energies, and nuclear decay energies for comparison with various nuclear models and predictions. Among neutron-deficient actinides, which are characteristically unstable toward decay by α-particle emission and EC, such investigations can often be conveniently carried out by α-spectrometry.

In the early 1990s, Andreyev *et al.* (Table I) were able to identify ^{230}Pu [4] and ^{229,228}Pu [5] among the irradiation products of ^{208}Pb bombarded with ^{24,26}Mg ions. The compound nucleus recoils were separated using the kinematic separator ''VASSILISSA'' and were directly implanted into silicon strip α-detectors to measure their decay. This method provides a reliable measurement of the α-particle energies, but it is not able to measure the half-life of isotopes that have half-lives longer than the time intervals of about 0.2 s between random events in their detectors. Half-lives for ^{230,229,228}Pu were predicted to be about 200, 10, and 2 s [6], respectively, and would be too long for this type measurement. The half-life for ^{231}Pu [7] was expected to be in the range of 3 to 30 min, which is also too long for VASSILISSA experiments, but ideal for on-line chemical separations.

Andreyev *et al.* [4] measured a production cross section of 100 nb for the ^{208}Pb(^{26}Mg,4n)^{230}Pu reaction, and the ^{208}Pb(^{26}Mg,3n)^{231}Pu cross section is expected to be smaller. Consequently, we chose the ^{233}U(^{3}He,5n) reaction for production of ^{231}Pu over the ^{208}Pb(^{26}Mg,3n) reaction because the expected ^{231}Pu production rate was higher. In our earlier investigations of the ^{233}U(^{3}He,4n) reaction [8], we measured a ^{232}Pu cross section of (5.0 ± 0.5) μb for 36-MeV projectiles. This value is two orders of magnitude lower than obtained from the JORPLE [9] computer code, which has predicted cross sections in reasonable agreement with experiments for neutron evaporation reactions of heavy target nuclei with heavier projectiles. JORPLE calculates a maximum cross section of 20 μb for the ^{231}Pu production via the ^{233}U(^{3}He,5n) reaction.

In light ion-induced reactions the compound nucleus products have recoil ranges of only a few tens of μg/cm^2, limiting the effective target thickness and, consequently, the production rate. Therefore, the approach of complete target dissolution and subsequent chemical separation of the pro-

TABLE I. Summary of decay data for neutron-deficient plutonium isotopes sorted by reference.

Reference	Pu isotope	Half-life	E_α (MeV)
Orth [1]	232	36 ± 2 min	6.58
	234	9.0 ± 0.5 h	6.19 ± 0.01
Thomas *et al.* [2]	233	20 ± 2 min	6.30 ± 0.02
Jäger *et al.* [3]	232	34.1 ± 0.7 min	6.600 ± 0.010
			6.542 ± 0.010
	233	20.9 ± 0.4 min	
	234	8.8 ± 0.1 h	6.151
			6.202
Andreyev *et al.* [4,5]	230		7.050 ± 0.015
	229		7.46 ± 0.03
	228		7.81 ± 0.02

*Present address: Institut für Kernchemie, FB 15, Philipps-Universität Marburg, Hans-Meerwein-Strasse, D-35043 Marburg/Lahn, Germany.

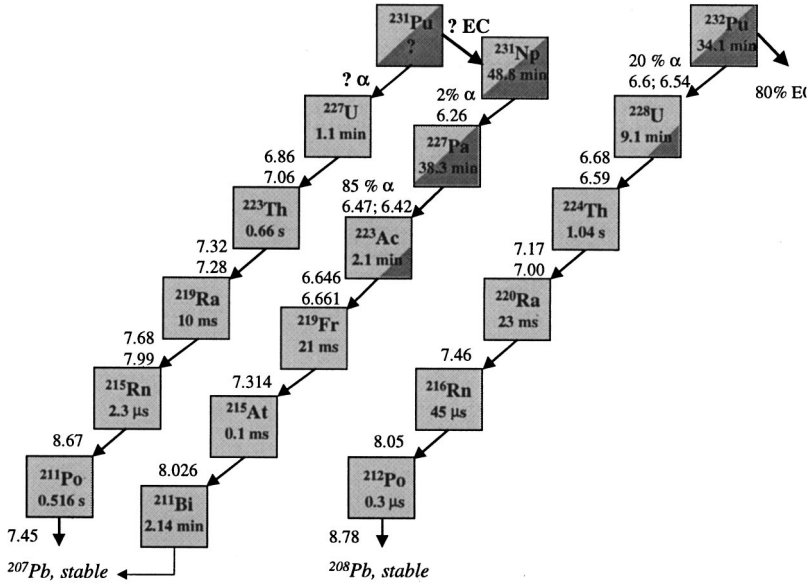

FIG. 1. Decay chains from the decay of ^{231}Pu and ^{232}Pu, the most abundant plutonium isotopes. The chains resulting from both the α-decay and EC-decay of ^{231}Pu are shown.

duced isotopes caught in the heavy target was used in the earlier plutonium investigations [1–3]. These heavy targets were made of either uranium metal or oxide. The recoil technique was developed for use in the search for short-lived isotopes, and to avoid dissolution of rare actinide targets. Products of the nuclear reactions recoil out of the target and are either caught in thin foils (''catcher'' foils) placed close to the target or on aerosols transported in a flowing gas stream. A special Light Ion Multiple (LIM) target system, using an array of many very thin targets, was designed by H. L. Hall [10] to overcome the disadvantages of the short recoil ranges associated with light ion-induced reactions.

An additional difficulty resulting from the use of the ^{233}U(^{3}He,xn)$^{236-x}$Pu reaction is the interference from products of other reactions, primarily, charged-particle emission. These reactions result in high production rates of neptunium, uranium, and thorium isotopes. Therefore, plutonium has to be chemically separated from them, because their decay interferes strongly with the measurement of the α-decay of ^{231}Pu. The main challenge in the ^{231}Pu identification process was, consequently, to find an efficient and fast chemical separation for plutonium. Early attempts [11] using either extraction with thenoyl-tri-fluoroacetone (TTA) or anion exchange to separate plutonium failed. The stringent requirements for purity, speed, and yield could not be achieved. These requirements prompted the development of a novel separation procedure based on the principle of solid phase extraction.

Another challenge in studying ^{231}Pu arose from the difficulty of observing the EC-branch. ^{231}Np, the direct EC-daughter of ^{231}Pu, decays by α-emission with only a 2% branch, thus, 98% of the EC-decay is unobservable via α-spectrometry. Furthermore, the intensity of the α-decay from the EC-branch is only 1.7% because ^{227}Pa, the daughter, decays with only an 85% α-branch. The low α-decay rate, in conjunction with the relatively long half-lives of these isotopes, 48.8 min and 38.3 min, respectively, makes detection of the EC-branch exceedingly difficult.

The complexity becomes clear by looking at the decay chains of the plutonium isotopes of interest shown in Fig. 1. In earlier attempts, the similar α-decay energies of the daughter isotopes, their relatively long half-lives, and their initial simultaneous direct production prevented the identification of ^{231}Pu. In the present study, more selective chemical separation and sensitive α-α-correlation detection techniques were used to overcome these experimental difficulties.

II. EXPERIMENTAL

A. Production

Neutron-deficient plutonium isotopes were produced in irradiation of ^{233}U with ^{3}He^{2+} ions. The targets [12] consisted of ^{233}U (4.2 ppm ^{232}U deposited on Be disks (4.6 mg/cm^2) by molecular plating and converted to the oxide. The effective target areas were 0.28 cm^2 (diameter 6 mm), and target thicknesses ranged from 48 to 80 μg/cm^2 of ^{233}U. The targets were mounted on aluminum frames, which fit into the LIM target system [10]. Eleven targets, 6 mm apart, were arranged in the LIM target system. The beam entrance vacuum window of the target system and the volume limiting foil after the last target were 4.6 mg/cm^2 Be-foils. The 48-MeV ^{3}He^{2+} beam was provided by the 88-Inch Cyclotron at the Lawrence Berkeley National Laboratory. The beam energies ranged from 47.1 MeV (lab system) in the first target to approximately 42.2 MeV in the eleventh target of the LIM array. The ^{3}He^{2+} beam intensity was 8-10 $e\mu$A.

The reaction products recoiling out of the targets were continuously removed from the production site by the He/KCl aerosol gas transport system. The recoiling reaction products stop in the helium atmosphere and attach to the aerosols in the helium stream (flow rate 3 L/min), which sweeps out the volume behind each target. The activity-laden aerosols are transported via a 2-mm-i.d. Teflon capillary to the collection site, a manually rotatable four position wheel inside a fume hood located 9 m from the target system outside the concrete shielding. At the collection site, the reaction product bearing aerosols were collected on platinum foils under vacuum. After a collection period of 10 minutes,

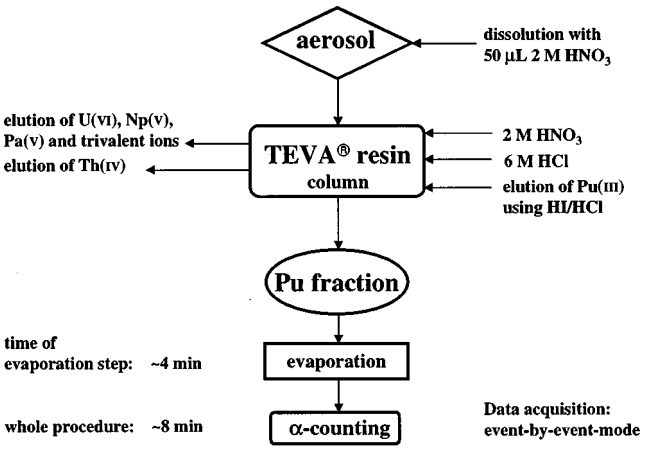

FIG. 2. Flow chart of the solid phase extraction procedure for separation of plutonium from interfering neighboring elements.

the wheel-collection system was let up to air, and the wheel was rotated to remove the collected sample.

B. Chemical separation

The KCl aerosol was dissolved in dilute nitric acid and chemically processed to separate plutonium from interfering reaction products, including neptunium, uranium, protactinium, thorium, etc., formed directly as well as by decay of the plutonium isotopes during irradiation/collection time. The chemical separation is based on a solid phase extraction procedure using TEVA-resin (EIChroM Industries), a quaternary amine salt—a strong anion exchanger. The chemical procedure is outlined as a flow chart in Fig. 2. The aerosol was taken up in 50 μL 2 M nitric acid containing ^{239}Pu as a chemical yield tracer. The solution was transferred to a 2-mm-i.d. column packed 2 cm in height, resulting in a free column value of 50 μL. The column was rinsed with 2.5 mL 2 M nitric acid, followed by 3 mL 6 M HCl. Finally, 250 μL of a mixture of concentrated HCl and HI (volume ratio 9:1) was used to elute plutonium by reduction to Pu(III). The eluate was collected directly on a platinum disk on top of a hot plate. As soon as the sample was evaporated, the sample disk was flamed and placed on a solid state α-detector. Purification takes about 4 minutes and evaporation another 4 minutes; thus, a total of 8 minutes elapsed between end of collection (end of bombardment) and start of α-counting. The separation procedure will be described in detail elsewhere [13]. The purified plutonium samples were assayed via α-spectrometry. Each sample was counted for approximately 2 hours. Repeated cycles of collection, separation, and α-counting were performed in order to obtain statistically significant and reliable results.

C. Detection system

Thirteen PIPS (passivated ion implanted silicon) detectors were used; each having an active area of 300 mm^3 and a counting efficiency of 36%. A full width at half maximum (FWHM) of 25 keV was obtained for the 6.062 MeV ^{212}Bi and 8.784 MeV ^{212}Po lines of the ^{212}Pb source used for energy calibration. The FWHM for the ^{239}Pu line at 5.157 MeV, which serves as an internal tracer, was 80 keV under experimental conditions due to energy degradation in the samples.

Incoming signals from the PIPS detectors, after appropriate amplification and pulse shaping, were digitized to 11-bit (2048 channel) accuracy by analog-to-digital converters (ADC) in a CAMAC crate. Detector number, ADC-channel number, and time of detection (in milliseconds from a 10 MHz clock) of each α-particle were recorded in list mode. Beam intensities, collection times, separation times, and times for the beginning and end of measurement for each sample were also recorded. The CAMAC create controller and CAMAC instruction list processor were driven with Chaos data acquisition and analysis software [14]. ADC conversion and CAMAC readout resulted in a dead time of 110 μs for each event.

D. Data analysis

The data stored in list mode were sorted to produce (a) histograms of the numbers of α-counts versus their energy and (b) lists of α-α-correlations between parent and daughter decays. The list of α-α-correlations was sorted according to given criteria such as parent α-energy, daughter α-energy, time of occurrence of parent decay, and time interval between parent and daughter decay. The data for the decay curves, which were fit with the MLDS (maximum likelihood decay by simplex method) [15] code, were obtained by sorting parent-daughter correlations after the time of occurrence of the specific parent decay within a certain time interval between parent and daughter decay.

III. EXPERIMENTAL RESULTS

Identification of ^{231}Pu was accomplished by observing the α-decay of members of its α-decay branch using the α-α-correlation technique. The α-spectra of purified plutonium fractions show a few sets of decay chains originating from plutonium isotopes. The spectra shown in Fig. 3 are summations of individual spectra of 30 plutonium samples prepared during the experiment. The first four 10-minute intervals of the 2-h-acquisition time are shown. Within the first two time intervals, the decay of the ^{231}Pu α-branch can clearly be observed. The α-group positions from members of the ^{231}Pu α-decay chain are given in Fig. 3(a). The intensity of specific daughter groups, 7.3 MeV of ^{223}Th, 7.68 and 7.99 MeV of ^{219}Ra and 8.67 MeV of ^{215}Rn decrease with time indicating a half-life in the 10-minute range. The ^{231}Pu α-decay group is not obvious in the spectra because it is obscured by other peaks. The EC-branch of ^{231}Pu [daughter isotopes are shown in Fig. 3(b) by indicating their α-group positions] is difficult to identify in the singles α-spectra due to the low abundance, as noted above. ^{232}Pu and the growth of its α-decay daughters dominate the spectra at all times. Comparing the intensities of the α-groups from ^{224}Th (7.17 MeV), ^{220}Ra (7.45 MeV), ^{232}Pu (6.60 MeV) and ^{228}U (6.68 MeV) within the 10-minute intervals shows that the ^{232}Pu α-decay chain is close to equilibrium 20 to 30 minutes after the start of measurement, e.g., about 24 minutes after separation. This is indicated in Fig. 3(c). The α-groups belonging to the ^{232}Pu α-decay chain are labeled in Fig. 3(d).

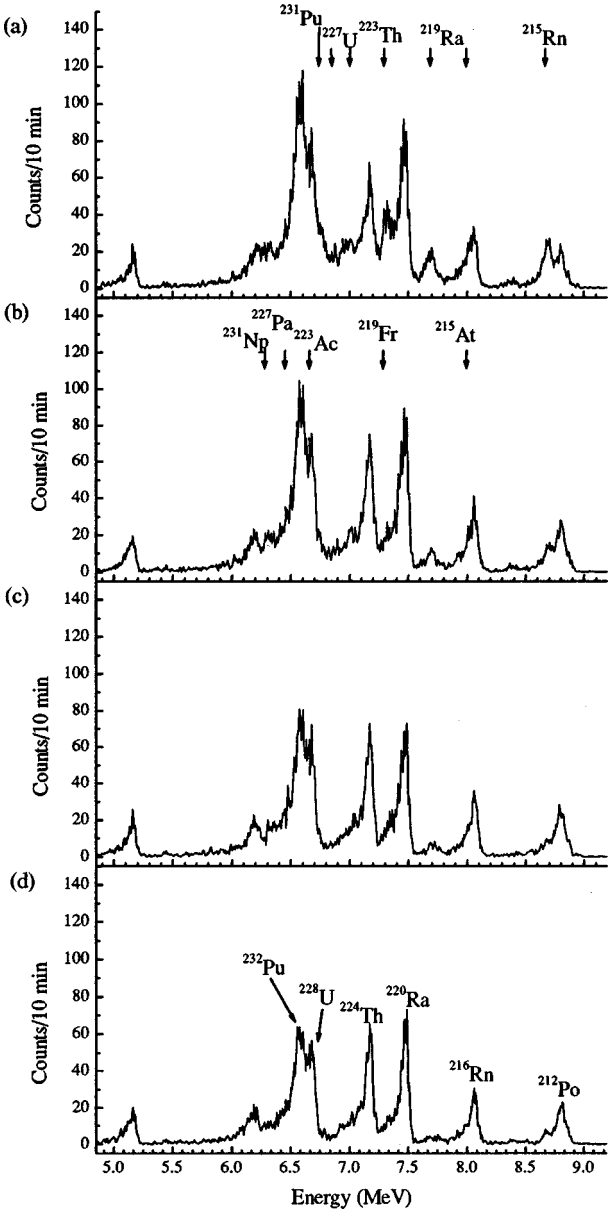

FIG. 3. Singles α-spectra, the summation of 30 separately purified plutonium samples. The spectra (a) to (d), are four consecutive 10-minute measurements. The spectra are dominated by the ^{232}Pu α-decay chain members, which are indicated in (d). The α-decay groups of the ^{231}Pu decay chains members are partially obscured by ^{232}Pu daughters. The positions of the α-groups resulting from the α- and EC decay of ^{231}Pu are shown in (a) and (b), respectively.

An unequivocal identification of ^{231}Pu, its decay chains, as well as α-decay chains in general, could only be made by applying the α-α-correlation technique. Figures 4 and 5 present the α-α-correlation data. Every pair of α-events occurring within a preselected parent-daughter time interval (time interval between parent and daughter decay) is plotted as a point with the first event (parent energy) along the abscissa and second event (daughter energy) along the ordinate. Selection of the parent-daughter time interval, together with the parent and daughter energies, provides a powerful method for identification of specific isotopes or decay chains. Measurement of times of occurrence of the decay chains relative to the start of counting can be used to determine the

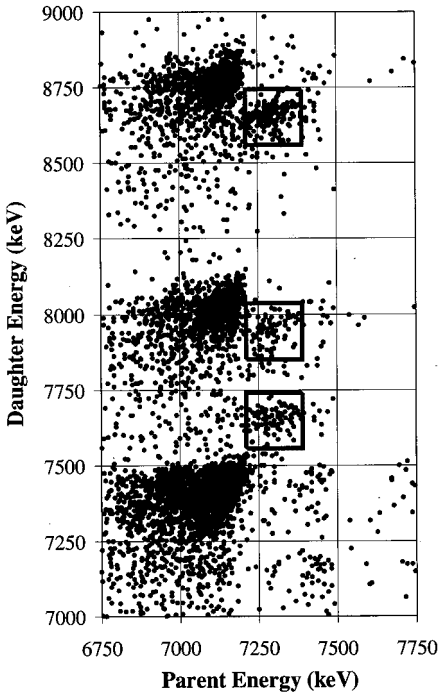

FIG. 4. α-α-correlations detected in the parent-daughter time interval (PDTI) $2<\mathrm{PDTI}<40$ ms of all 30 purified plutonium samples. Regions of correlations due to the α-decay branch of ^{231}Pu are indicated by rectangles. A total of 380 correlations within the energy windows of 7.2–7.4 MeV for the ^{223}Th parent, 7.55–7.74 MeV, 7.86–8.05 MeV for the ^{219}Ra daughter and 8.55–8.74 MeV for the ^{215}Rn daughter were used for the half-life analysis.

half-life of long-lived isotopes at the beginning of α-α-decay chains.

By choosing an optimal parent-daughter time interval (PDTI), chains of interest can be identified by the occurrence of their specific correlations. PDTIs greater than 500 ms can often not be analyzed because of the increasing effect of random correlations. Thus, the α-α-correlation technique is limited to short-lived daughters of α-decay chains. It should be noted, that, because of the 110 μs conversion and readout time α-α-correlation with PDTIs less than this dead time cannot be recorded.

The parent half-life is easy to obtain from correlation data, because an α-decay chain is fed with the half-life of the parent. The half-life determination is a necessary cross check to ensure that observed correlations really belong to the decay chain of the parent of interest and not to the chain of simultaneously produced daughters, or to random correlations.

Figure 4 shows α-α-correlations for PDTI of 2 ms $<\mathrm{PDTI}<40$ ms. Dominating in this plot, as well as in the α-singles spectra already shown, is the α-decay chain of ^{232}Pu. The starting point for ^{232}Pu correlations is the ^{224}Th granddaughter with its groups at 7.0 MeV and 7.17 MeV, representing here the parent for the correlations. ^{224}Th (1.04 s) decays to ^{220}Ra (7.46 MeV, 23 ms) to ^{216}Rn (8.05 MeV, 45 μs) and further to ^{212}Po (8.78 MeV, 0.3 μs). A half-life check proved that ^{232}Pu is the parent of the observed chain.

Nevertheless, the correlations essential for the identification of ^{231}Pu are indicated in Fig. 4 by shaded boxes as a guidance. The starting point for this correlation chain was

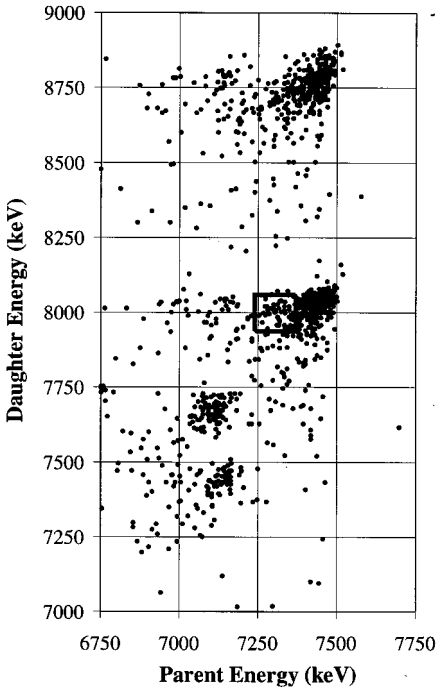

FIG. 5. α-α-correlations detected in parent-daughter time interval $0<\mathrm{PDTI}<1$ ms of all 30 purified plutonium samples. Correlations of the last members of the ^{232}Pu α-decay chain dominate the plot, but the area within the small box shows the important region for the unequivocal identification of the ^{231}Pu EC-branch. The correlations in this area represent the last members of the ^{231}Np α-decay chain, the EC-daughter of ^{231}Pu. A total of 30 correlations were counted within the energy region of 7.25–7.34 MeV for the ^{219}Fr parent and 7.97–8.06 MeV for the ^{215}At daughter.

identified to be ^{223}Th (0.66 s), the granddaughter of ^{231}Pu, whose α-decay energies range from 7.28 to 7.46 MeV. Observation of the characteristic intensity pattern of the α-groups of its daughter ^{219}Ra (66%–7.68 MeV and 33%–7.99 MeV, 10 ms), decaying to ^{215}Rn (8.67 MeV, 2.3 μs) proved the presence of the assumed α-decay chain. A half-life analysis based on these correlations, as shown later, indicated that ^{231}Pu has to be the parent of the observed chain.

Based on this result, the correlation data were examined in order to see if the EC-branch of ^{231}Pu could be found. The only possible correlation for unequivocal detection of the EC-branch of ^{231}Pu (see also Fig. 1) is the correlation between the last chain members, ^{219}Fr (7.314 MeV, 21 ms) decaying to ^{215}At (8.026 MeV, 0.1 ms). Based on the half-life of the 0.1 ms daughter, ^{215}At, the expected correlations should most likely be found within a PDTI of less than one millisecond. The correlation plot of this PDTI is shown in Fig. 5. A shaded box indicated the area of the correlations of the last chain members of the ^{231}Pu EC-branch. Although the plot is dominated by ^{232}Pu chain correlations, they do not interfere strongly because the energy limits were set from 7.25–7.34 MeV for ^{219}Fr and 7.97–8.06 MeV for ^{215}At. The small number (30) of detected correlations for the ^{231}Pu EC-branch reflects the fact that only 1.7% of the electron-capture process results in α-decays.

The correlations of the α-decay branch of ^{231}Pu (Fig. 4) are the basis of the ^{231}Pu half-life determination. Figure 6 shows the decay-curve analysis for the parent half-life based

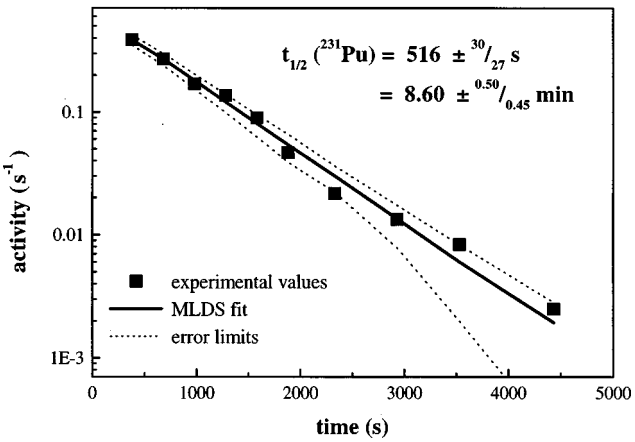

FIG. 6. Decay curve analysis for the 380 α-α-correlations assigned to the decay chain of ^{231}Pu performed by MLDS [15].

on the correlations which are assigned to the α-decay chain of ^{231}Pu. A total of 380 correlations detected within the energy windows of 7.2–7.4 MeV for the ^{223}Th parent energy, 7.55–7.74 and 7.86–8.05 MeV for the ^{219}Ra daughter energies, and 8.55–8.74 MeV for the ^{215}Rn daughter energy were used in the half-life analysis. Correlations with a parent energy higher than 7.4 MeV were not taken into account for the analysis because of interferences from the 7.45-MeV group due to the decay of ^{220}Ra, a member of the ^{232}Pu α-decay chain. The number of α-α-correlations in the ^{231}Pu α-decay chain was corrected for a minor contribution due to random correlations of unrelated α-decays. The number of random correlations for a given parent-daughter pair was estimated by counting random correlations in which daughter energies preceded parent energies. The correction amounted to 6 of the 380 correlations. The half-life analysis was performed using MLDS [15]. The straight line in Fig. 6 is the maximum likelihood fit to the data points, and the dashed lines represent a 68%-probability interval about the fit. From this analysis, the half-life of ^{231}Pu was determined to be (8.6 ± 0.5) min, where the error limit represents a 68%-confidence interval.

The initial activities for both decay branches of ^{231}Pu for the 30 10-minute collections were determined by MLDS [15], and accordingly corrected for efficiencies, for daughter α-decay branches, for pulse pile-up in the ADC gate, and for events missed during ADC conversion and readout time. The initial activities for the α- and the EC-branch of ^{231}Pu are (5.8 ± 0.6) s^{-1} and (51.4 ± 15.7) s^{-1}, respectively. The values for the α- and EC-decay branches are determined to be (10^{+7}_{-3})% and (90^{+3}_{-7})%, respectively, under the assumption that only these decay modes occur. The uncertainty in the number of α-α-correlations from ^{231}Pu EC-branch dominates the error limits on the decay branch intensities, which were calculated by evaluating the upper and lower limit of the initial activities.

The total half-life for ^{231}Pu, together with α- and EC-branches, yielded a partial half-life for α-decay of (86^{+36}_{-28}) min. Using the Hatsukawa systematics [6], the most likely ^{231}Pu α-decay energy region is 6.7–6.8 MeV. A careful analysis of this region in the singles α-spectra showed that there is a high energy shoulder at $\sim$6.72 MeV in the region

of the ^{232}Pu and ^{228}U groups, that is most likely due to α-decay of ^{231}Pu (Fig. 3). The shoulder is masked by ^{232}Pu and ^{228}U, but a two-component decay analysis gives a half-life of 8 to 10 min, which is consistent with the decay of the daughter isotopes which are in equilibrium with ^{231}Pu. In addition, the initial activity of the $\sim$6.72 MeV α-decay is consistent with those of the daughter isotopes. The possibility that the $\sim$6.72 MeV activity is due to 9-min ^{228}U, the daughter of 34-min ^{232}Pu, can be excluded because the chemical separation of plutonium and uranium was essentially complete, so the ^{228}U activity should be in equilibrium with ^{232}Pu. This is inconsistent with the rapid disappearance of the $\sim$6.72 MeV high energy shoulder, as shown in Fig. 3.

From these data, the cross section for the production of ^{231}Pu in the ^{3}He + ^{233}U reaction at 42.2–47.1 MeV was estimated to be 130 nb. This cross section is only accurate to within a factor of three due to large uncertainties in the effective target thickness (recoil range of ^{231}Pu in U_3O_8) and the gas-jet transport efficiency.

IV. SUMMARY AND CONCLUSIONS

^{231}Pu was positively identified. The half-life was determined to be (8.6 ± 0.5) min from analysis of the α-α-correlations of the ^{223}Th, ^{219}Ra, and ^{215}Rn daughters of its α-decay branch. An α-group with an energy of (6.72 ± 0.03) MeV was identified in the singles spectra and assigned to ^{231}Pu.

The ratio of α- to EC-decay was determined to be 0.11 ± 0.05. Assuming no other decay modes occur, the abundance of the α- and EC-decay modes were evaluated to be (10^{+7}_{-3})% and (90^{+3}_{-7})%, respectively. Although the seemingly more intense α-decay branch dominates the identification process, ^{231}Pu decays primarily by EC. The reason for the small number of events in the EC-branch, which can be seen via the α-α-correlation technique, is the low abundance of only 2% for the α-decay branch of the first EC-daughter, ^{231}Np.

A logft value of 5.3 was calculated for the EC-decay of ^{231}Pu from the predicted Q_{EC} of 2820 kev, based on masses given by Audi *et al.* [7], and the experimentally determined half-life. This logft indicates that the EC-decay of ^{231}Pu is allowed with $\Delta\pi = no$ and $\Delta I = 0, \pm 1$. The $\frac{3}{2}^+$ ^{231}Pu ground state proposed by Audi *et al.* [7] is consistent with this logft value and the assumption of decay directly to the $\frac{5}{2}^+$ ground state in ^{231}Np [7,16].

The measured partial α-half-life of ^{231}Pu is (86^{+36}_{-28}) min and the theoretical partial α-half-life is 72.4 min as calculated via Hatsukawa systematics [6]. An α-decay hindrance factor of (1.8 ± 0.7) is calculated by assuming that approximate α-branching to the $\frac{3}{2}^+$ ground state of ^{227}U is about the same as the 65% population of the analogous state in ^{225}Th from ^{229}U decay [16,17]. The low hindrance factor implies that the observed ^{231}Pu α-decay is a favored transition.

The $\frac{3}{2}^+$ ground state favored by Audi *et al.* [7] for ^{231}Pu is presumably the $\frac{3}{2}^+[631]$ single particle state, which is also the ground state of the ^{229}U isotone [17]. Interestingly, ^{227}U has also the $\frac{3}{2}^+$ ground state [7,16], indicating a level crossing between $N=135$ and $N=137$. Therefore, the observed ^{231}Pu α-decay probably represents a favored decay directly to the ground state of ^{227}U. This is completely analogous to the decay of the ^{229}U $\frac{3}{2}^+[631]$ to the ^{225}Th $\frac{3}{2}^+[631]$ ground state [17]. In addition, the assignment of $\frac{3}{2}^+[631]$ to the ground state in ^{231}Pu is in agreement with Nilsson diagrams at $N=137$ [16] at the deformation of $\varepsilon_2=0.183$ calculated by Möller *et al.* [18].

Interpreting the 6.72 ± 0.03 MeV α-group of ^{231}Pu as decay to the ground state in ^{227}U and using the masses of ^{227}U and ^{4}He given by Audi *et al.* [7], a Q-value for the α-decay of (6.838 ± 0.030) MeV and a mass excess of (38.270 ± 0.035) MeV for ^{231}Pu were calculated. The determined mass excess is in good agreement with the evaluations of 38.430 MeV by Audi *et al.* [7], 38.310 MeV by Möller *et al.* [18], 38.330 MeV by Dussel *et al.* [19]. The atomic mass of ^{231}Pu was calculated to be (231.04108 ± 0.00004) u from our experimental mass excess value.

ACKNOWLEDGMENTS

This work was supported in part by the Office of Energy Research, the Office of Basic Energy sciences, Chemical Sciences Division, and the Office of High Energy and Nuclear Physics, Nuclear Physics Division of the U.S. Department of Energy under Contract DE-AC03-76SF00098. We also wish to thank the Alexander von Humboldt Foundation for providing partial funding for Dr. Carola A. Laue and the German Academic Exchange Service, DAAD, for the financial support of Ralf Sudowe.

[1] D. A. Orth, Ph.D. thesis, University of California, Berkeley, 1951; University of California Radiation Laboratory Report UCRL 1059, 1951 (unpublished).

[2] T. D. Thomas, R. Vandenbosch, R. A. Glass, and G. T. Seaborg, Phys. Rev. **106**, 1228 (1957).

[3] U. Jaeger, H. Muenzel, and G. Pfennig, Z. Phys. **258**, 337 (1973).

[4] A. N. Andreyev, D. D. Bogdanov, V. I. Chepigin, A. P. Kabachenko, S. Sharo, G. M. Ter-Akopian, and A. V. Yeremin, Z. Phys. A **337**, 231 (1990).

[5] A. N. Andreyev, D. D. Bogdanov, V. I. Chepigin, A. P. Kabachenko, O. N. Malyshev, A. G. Popeko, R. N. Sagaidak, G. M. Ter-Akopian, M. Vesesky, and A. V. Yeremin, Z. Phys. A **347**, 225 (1994).

[6] Y. Hatsukawa, H. Nakahara, and D. C. Hoffman, Phys. Rev. C **42**, 674 (1990).

[7] G. Audi, O. Bersillon, J. Blachot, and A. H. Wapstra, Nucl. Phys. **A626**, 1 (1997).

[8] C. A. Laue, K. E. Gregorich, J. A. Adams, M. R. Lane, D. M. Lee, C. A. McGrath, D. A. Shaughnessy, D. A. Strellis, E. R. Sylwester, and D. C. Hoffman, Lawrence Berkeley National Laboratory, 1997 Annual Report Nuclear Science Division, LBL 39764, N27, 1998 (unpublished).

[9] J. Alonso, *Gmelins Handbuch der Anorganischen Chemie*

(Verlag Chemie GmbH, Weinheim, Germany, 1973), Band 7b, Part A1.

[10] H. L. Hall, M. J. Nurmia, and D. C. Hoffman, Nucl. Instrum. Methods Phys. Res. A **276**, 649 (1989).

[11] C. A. Laue, K. E. Gregorich, J. A. Adams, M. R. Lane, D. M. Lee, C. A. McGrath, D. A. Shaughnessy, D. A. Strellis, E. R. Sylwester, P. A. Wilk, and D. C. Hoffman, Lawrence Berkeley National Laboratory, 1997 Annual Report Nuclear Science Division, LBL 39764, N26, 1998 (unpublished).

[12] S. A. Kreek, H. L. Hall, K. E. Gregorich, R. A. Henderson, J. D. Leyba, K. R. Czerwinski, B. Kadkhodayan, M. P. Neu, C. D. Kacher, T. M. Hamilton, M. R. Lane, E. R. Sylwester, A. Türler, D. M. Lee, M. J. Nurmia, and D. C. Hoffman, Phys. Rev. C **50**, 2288 (1994).

[13] C. A. Laue, R. Sudowe, K. E. Gregorich, and D. C. Hoffman (in preparation).

[14] W. H. Rathbun, Lawrence Berkeley National Laboratory Report, LBL-29734, 1991 (unpublished); W. H. Rathbun, K. E. Gregorich, and M. F. Mohar, Lawrence Berkeley National Laboratory, 1993 Annual Report Nuclear Science Division, LBL-35768, 82, 1994 (unpublished).

[15] K. E. Gregorich, Nucl. Instrum. Methods Phys. Res. A **302**, 135 (1991).

[16] *Table of Isotopes*, 8th ed., edited by R. B. Firestone and V. S. Shirley (Wiley, New York, 1996), Vol. II.

[17] *Table of Isotopes*, 7th ed., edited by C. M. Lederer and V. S. Shirley (Wiley, New York, 1978).

[18] P. Möller, J. R. Nix, W. D. Myers, and W. J. Swiatecki, At. Data Nucl. Data Tables **59**, 185 (1995).

[19] G. Dussel, E. Caurier, and A. P. Zuker, At. Data Nucl. Data Tables **39**, 185 (1988).